JMEPEG (2012) 21:707–713
DOI: 10.1007/s11665-012-0149-8

1059-9495/$19.00

Evaluation of Corrosion Performance of Titanium/Steel Joint Brazed by Cu-Based Filler Metal

A. Elrefaey, L. Wojarski, and W. Tillmann

(Submitted October 20, 2011; in revised form January 2, 2012)

Furnace vacuum brazing has been employed to join commercially pure titanium and low carbon steel using copper-based filler metal with the composition of Cu-10.6Mn-1.9Ni, at.%. Three different brazing temperatures 930, 970, and 1000 °C and a holding time of 15 min were studied and evaluated. The corrosion behavior of the joint in 0.1 M sulfuric acid was investigated using immersion and electrochemical tests. Measurements of corrosion potential, corrosion current density, corrosion rate, polarization resistance, weight loss, and morphology of corrosion attack were used in this study. Experimental results showed that severe corrosion attack of the steel side at the interfacial area is clearly observed. Despite the difference in corrosion rate values obtained by electrochemical and weight loss measurements, the trend of results was identical to a large extent. Corrosion resistance of the joint showed a general tendency to increase with rising brazing temperature. The lowest corrosion rate was obtained for the couple bonded at 1000 °C. Meanwhile, at the lowest joining temperature of 930 °C, corrosion rate showed a higher value. The results of joints corrosion resistance were attributed to the difference in microstructure features and chemical analysis.

Keywords brazing, corrosion, steels, titanium

1. Introduction

Titanium alloys with excellent specific tensile and corrosion resistance have been mainly used for nuclear and chemical industry, as materials for petrochemical plants and surgical implants (Ref 1-3). When pressures and/or temperatures and size demand a very thick plate, the titanium equipment can become considerably more expensive than units constructed from lower performance materials (Ref 4). Thus, there was a considerable interest in joining titanium to low-cost materials such as steel alloys. Unfortunately, titanium and steel exhibit poor metallurgical compatibility, which promotes the formation of brittle intermetallic phases such as Fe-Ti and Ti-C. Therefore, it is apparent that the ability to weld these materials is the key to making them more attractive.

The difficulty of bonding of titanium to other metals could be relieved by using brazing techniques. Brazing is beneficial because it involves the melting of the filler material only, thus eliminating problems that occur when fusing dissimilar metals. Moreover, brazing enables joining many dissimilar metals without severe distortion, and so this process has been widely used for these applications.

Detailed investigation of titanium to steel joints using copper-based alloy (Cu-10.6Mn-1.9Ni, at.%.) was separately performed by the authors. Optimal brazing temperatures, the temperatures at which the best microstructure and mechanical properties were achieved, have been reached in the joint (Ref 5). Since the joint is composed of different materials (titanium, steel, and copper-based filler) and different structures and because of the change in the brazing cycle, a clear estimation of the corrosion resistance of this joint is becoming an essential criterion in evaluating the performance of the joint.

The objective of this investigation is focused on corrosion properties of the steel/titanium joint. The degradation behavior of the joint brazed at different cycles was analyzed and compared by means of electrochemical techniques, mass loss, and morphology of corrosion attack. This study also aims to explore the reasons for the change in corrosion resistance of the brazed joints.

2. Experimental Procedures

2.1 Specimen Preparation

Plates of commercially pure titanium (CP Ti) and low carbon steel were used for brazing with their chemical compositions listed in Table 1. The plates were cut into 10 mm × 10 mm × 2 mm chips and then prepared, using grinding papers with different stages up to 1000 grit, and were subsequently cleaned ultrasonically in acetone before brazing. The filler alloy is a 100-μm-thick Cu-10.6Mn-1.9Ni, at.% foil, which has a melting range of 970-990 °C. The brazing foil was cleaned in acetone before brazing and then sandwiched between a 6-mm overlapping area of base metals. The joints

This article is an invited submission to JMEP selected from presentations at the Symposia "Wetting, soldering and brazing" and "Diffusion bonding and characterization" belonging to the Topic "Joining" at the European Congress and Exhibition on Advanced Materials and Processes (EUROMAT 2011), held September 12-15, 2011, in Montpellier, France, and has been expanded from the original presentation.

A. Elrefaey, L. Wojarski and **W. Tillmann,** Lehrstuhl für Werkstofftechnologie, Technische Universität Dortmund, Leonhard-Euler-Str. 2, 44227 Dortmund, Deutschland. Contact e-mails: ahmed.elrefaey@udo.edu and elrefaey@gmail.com

Table 1 Chemical composition of the of the titanium and steel plates

	Chemical analyses, at.%									
Alloy	C	Fe	Ti	Mn	Si	P	S	N	H	O
CP Ti	0.08	0.03	Bal.	···	···	···	···	0.1	0.11	0.74
Low carbon ste	0.23	Bal.	···	0.17	0.02	0.07	0.02	···	···	···

Table 2 Brazing parameters used in the experimental study

Joint	Brazing temperature, °C	Soaking time, min
Ti/St-930-15	930	15
Ti/St-970-15	970	15
Ti/St-1000-15	1000	15

were fixed with a stainless steel clamp and then carefully placed into a vacuum furnace. Brazing experiments were carried out up to the parameters shown in Table 2. The heating and cooling rates were adjusted at 15 °C/min.

2.2 Microstructure Analyses

The cross sections of the bonded titanium/steel joints were prepared for metallographic analysis by standard polishing techniques and then etched by 5% HF, 20% HNO_3, and 75% glycerol solution for 60 s for titanium side, and by 3% Nital solution for steel side. The microstructures before and after the electrochemical characterization were investigated using a NICKON-EPIPHOT optical microscope. In addition, the morphology and standerless-chemical analyses of the joint, where the accuracy is within 5%, were evaluated by a JEOL JXA-840 scanning electron microscope equipped with an energy dispersive spectrometer (EDS).

2.3 Electrochemical Measurements

A glass cell was used for the electrochemical experiment at a laboratory temperature of 20 ± 2 °C. The degradation behavior of the joints and base metals was studied on cross sections, and for each condition, at least three samples were tested. The working electrodes were cut and metallographically prepared. The cross section was exposed to the degradation media, and the rest of the sample was masked with epoxy resin. The experimental procedure includes the open-circuit potential (OCP), (measurement of the corrosion potential as a function of time) and the potentiodynamic polarization experiments. OCP was monitored for 3600 s and potentiodynamic tests samples were polarized from −1500 mV down to OCP to 3000 mV above OCP at a scan rate of 2 mV/s. The selected degradation media was 0.1 M sulfuric acid and the potentials were measured against Ag/AgCl/Sat. KCl electrode. Platinum electrode, with an exposed area of 4 cm^2, was used as counter electrode.

2.4 Immersion Tests

The immersion tests of brazed joints were conducted at 20 °C in a 6% $FeCl_3$ solution. The exposed cross-sectional area of all joints to the solution was almost 4 mm × 10 mm. The rest of the specimens were isolated by plastic especially used for these measurements. Before exposure, the samples were polished and cleaned with acetone, washed using distilled water, dried in air, and stored over a desiccant. The samples were weighed before the exposure for the original weight and then hung in test solutions for 24 h. After immersion at these times, the corroded specimens were removed from the solutions, cleaned with distilled water, and dried. Finally, the samples were weighed again to obtain the final weight

The depth of attack in the steel side and joint morphology were studied by using a 3D microscope with the accompanied software. The system initially scanned the specimen in multiple layers with adjusted extends. After completion of the scanning process, the 3D data were automatically loaded into the 3D viewer. It was then possible to rotate and tilt the 3D view and to make analysis measurements.

3. Results and Discussion

3.1 Microstructure Characterization Before Corrosion Tests

The brazing filler metal could not melt completely at a brazing temperature of 930 °C, and the voids were extensively formed especially at the middle of the brazed joint compared with the areas in contact with titanium and steel substrates, which showed melting and interaction of the brazed alloy with the two base metals, as shown in Fig. 1(a). This is attributed to the diffusion and dissolving of elements from the base metals into the brazing filler metal which lowers the melting temperature of this area compared to the bulk of brazing filler metal. At a brazing temperature of 970 and 1000 °C, sound joints were obtained since a homogeneous microstructure without voids or cracks was observed along the joint, as it is shown in Fig. 1(c) and (e).

Several interaction layers occur between the copper-based brazing alloy and the two substrates. According to Cu-Ti-Fe ternary phase diagram and up to the EDS analyses of different phases at the brazed area, copper solid solution (Cu), (Fe,Cu)Ti, Cu_4Ti_3, and α-β Ti phases were detected (Ref 6). Brazing temperature played a vital role in controlling the content and size of different phases at the brazed area. At a brazing temperature of 930 °C, a thin film of (Cu) was formed at the steel/Cu-based filler interfacial area (see Fig. 1b, area A). (Fe,Cu)Ti-based solid solution has quite high content of Cu, which was found close to the (Cu), (area B). Van Beek et al. (Ref 6) suggest that nearly 38 at.% Cu could be dissolved in FeTi. Substitution of Fe by Cu atoms leads to an expansion of the cubic lattice of TiFe. A similar behavior was found in the case of substitution of Ni by Cu atoms in the cubic lattice of TiNi (TiNi and TiFe are miscible at this temperature completely). In addition, Cu_4Ti_3 constituted the most of the brazed area, as indicated by area C, while thin α-β Ti layer was located at the titanium/Cu-based filler interfacial area (area D). Clear investigation of the microstructure has shown small isolated islands in the interior of brazed area as well (area E). The composition of these areas was more close to the phase $Ti45Cu_{55-x}Fe_x$, where $4 < x < 5$.

At a brazing temperature of 970 °C, α-β Ti layer was the main structure in the brazed region (area F), while (Fe,Cu)Ti compound, with higher content of copper, was formed at the steel/Cu-based filler interfacial area (see Fig. 1d, area G). At the

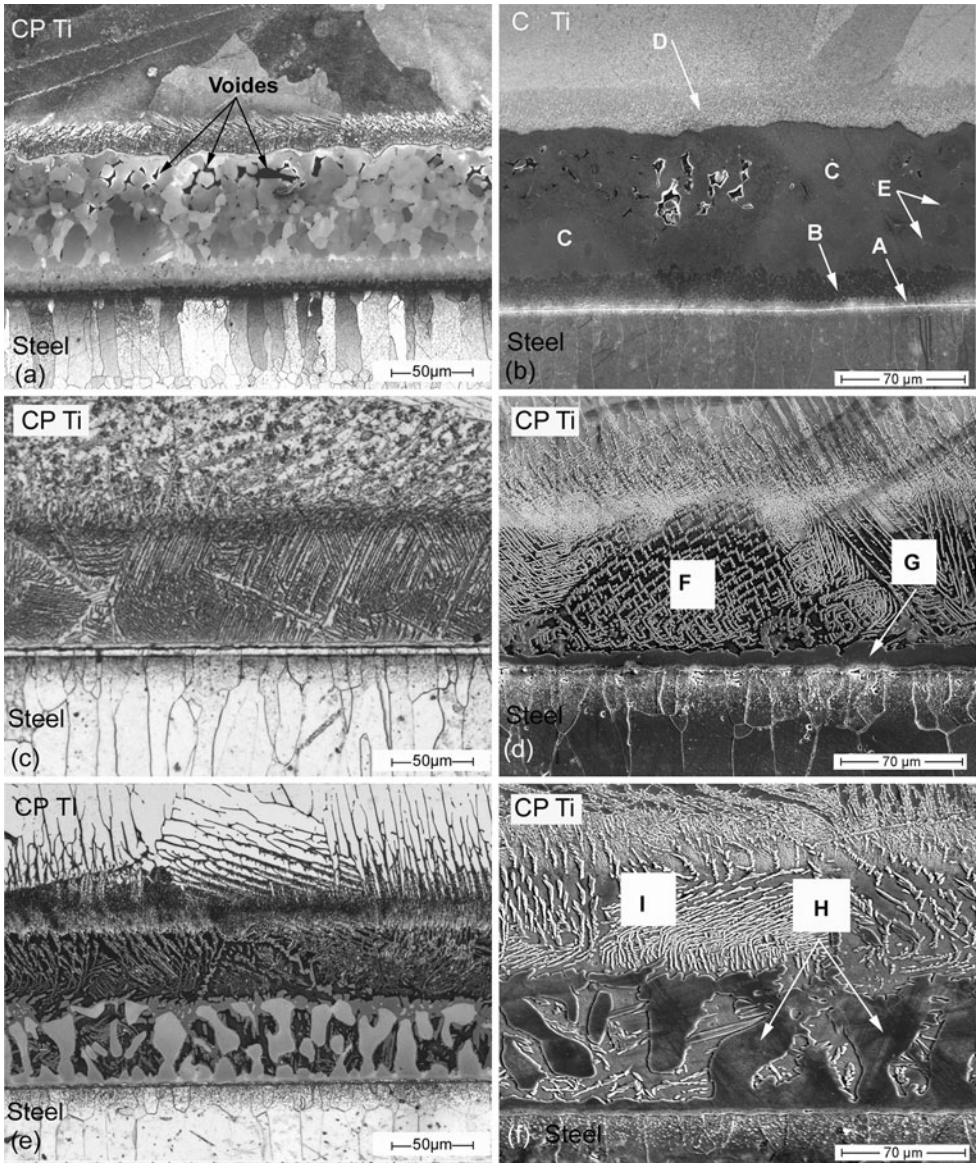

Fig. 1 Microstructure of brazed samples before corrosion tests: (a) optical microstructure of Ti/St-930-15 joint, (b) SEM micrograph of Ti/St-930-15 joint, (c) optical microstructure of Ti/St-970-15 joint, (d) SEM micrograph of Ti/St-970-15 joint, (e) optical microstructure of Ti/St-1000-15 joint, and (f) SEM micrograph of Ti/St-1000-15 joint

brazing temperature of 1000 °C, the (Fe,Cu)Ti compound was enlarged in size and constituted almost half of the brazed region (area H), meanwhile, α-β Ti layer formed in the other half (area I). Results of chemical analyses for the different areas together with the suggested phases were listed in Table 3.

Table 3 Chemical analyses at areas showed in Fig. 1

	Average chemical analyses, at.%					
Area	**Ti**	**Fe**	**Cu**	**Mn**	**Ni**	**Suggested phase**
A	06.0	05.4	80.1	08.5	···	(Cu)
B	46.9	26.8	21.5	03.9	0.9	(Fe,Cu)Ti
C	38.4	04.7	49.0	07.0	0.9	Cu4Ti3
D	86.5	05.1	07.1	1.3	···	α-β Ti
E	42.3	3.8	53.4	0.5	···	Ti45Cu55-*x*Fex
F	78.6	07.8	11.4	1.9	0.3	α-β Ti
G	47.3	20.9	29.9	1.5	0.4	(Fe,Cu)Ti
H	49	16.6	31.1	2.7	0.6	(Fe,Cu)Ti
I	71.9	09.2	15.5	3.1	0.3	α-β Ti

3.2 Degradation Behavior

The corrosion potential as a function of time for the titanium/steel joints at different brazing parameters and the base materials is shown in Fig. 2. It can be seen that after 3600 s, all the samples reach a stable OCP value. There is gab of potential in between titanium and copper-based foil at one side and the steel base metal together with all joints on the other side. The corrosion potentials were noble in case of the titanium and copper-based filler metal, while it showed active values in steel base metal and all brazed joints. Brazing at different thermal cycles resulted in a change of the microstructure in the brazed area, and the content of phases formed was different, as well. Nevertheless, the OCPs measured in the joint are quite similar. This means that all joints showed similar thermodynamic

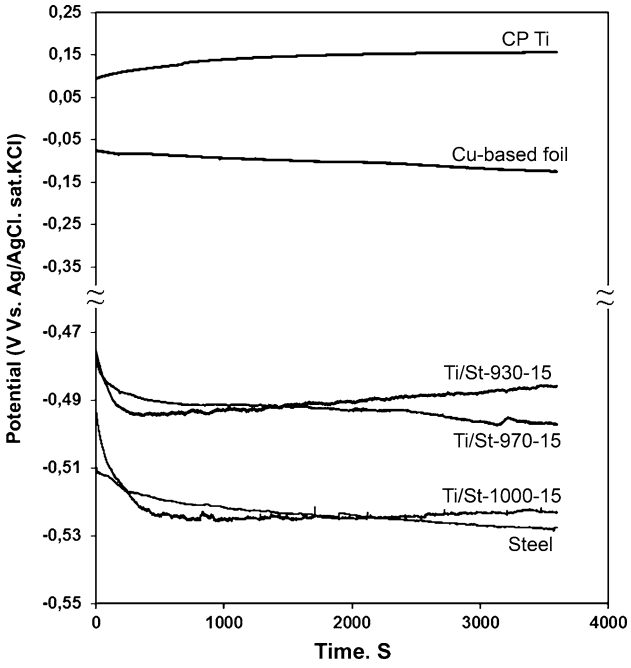

Fig. 2 Open circuit potential measurements for base metals and titanium/steel joints

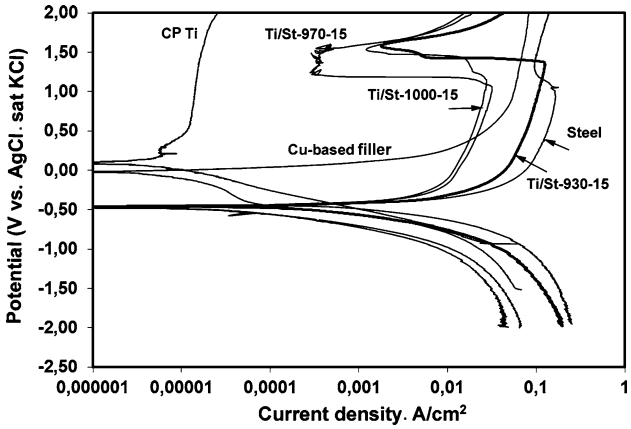

Fig. 3 Potentiodynamic polarization curves of base metals and brazed joints

tendency in the corrosion medium. This result is consistent with other literature (Ref 7, 8). A slight increase in the potential with time was observed in the titanium in contrast to the rest of the samples, which showed a small decrease of the potential, particularly at early stages of exposure. In general, an increase of the OCP with time is attributed to the formation and/or thickening of the passive layer and vice versa (Ref 9). The result suggests that the anodic part of the joint will be the steel side since it has the lowest potential. This may be beneficial to the joint since the brazed alloy has more positive potential than steel and the ratio of the cathodic to the anodic area is favorably low.

Quantitative information related to the kinetics of the corrosion reactions and the corrosion rate can be obtained from polarization curves. Figure 3 shows the anodic and cathodic polarization curves of the base metals and the brazed joints. There was almost no difference in the cathodic part of the curves. The only difference was in the anodic portion. As expected previously, titanium showed the best result in respect to a low current density (I_{corr}), a low current density of passivation, the large extension of its passive plateau, and at the same time, it showed the noblest E_{corr}. The joint Ti/St-1000-15 showed the second-best level of corrosion resistance after the titanium alloy which is much better than the other brazed joints and copper-based filler as well. Finally, the steel-based metal presented the lowest corrosion resistant material compared to all other samples. The joints brazed with different brazing parameters have shown a more or less similar behavior in terms of the corrosion potential, but with variation in the dissolution current density. The joint brazed at high temperature exhibited a better corrosion resistance than the one that was brazed at a lower temperature. It was also detected that the brazed samples, together with the steel-based metal, have shown active regions over a large range of potential. Meanwhile, there is no passivation observed after the active regions and only transpassive regions were detected.

The average of corrosion data obtained from corrosion tests are summarized in Table 4. The analyses of the corrosion parameters presented in the table corroborate the above referred comparative behavior. OCP and the potential at which $I = 0$ have shown very close values for each tested sample. These results indicate that the brazing temperature or the microstructure of the joints does not significantly modify the OCP and E ($I = 0$) values. In respect to corrosion kinetics, evaluated by the polarization resistance (R_p) and I_{corr}, the brazing temperature has influenced the results obtained. These results are coherent to those previously reported (Ref 8, 10). Analyses of the data have also shown that CP Ti presented the noblest value of E_{corr} and also the lowest I_{corr}, while steel showed an opposite behavior. In addition, I_{corr} and corrosion rate of the joint Ti/St-1000-15 is lower than all other joints. It is noted that there was a small difference in data listed in Table 4 and their corresponding measurements in Fig. 2 and 3. This difference is as a result of the calculation of the average of at least three measurements for the data in Table 4.

3.3 Microstructure Characterization After Corrosion Tests

The coupling of steel to titanium by copper-based filler metal leads to galvanic corrosion, and steel selectively and severely corroded since it is the anodic part of the joint. Localized attacks could clearly be seen in the steel side, directly in contact with copper-based alloy and titanium-based metal. The depths of the attacks varied owing to the used brazing parameters. Figures 4 and 5 show a comparison of the joints Ti/St-930-15 and Ti/St-1000-15, respectively. It is clear that the joint brazed at a temperature of 1000 °C has a lower depth of attack close to interfacial area than joints brazed at 930 °C. Furthermore, the high diffusion of the noble titanium element in the brazed area and the less noble copper element out of the brazed area helps to generally passivate the region. Consequently, the brazed area showed a lower attack than the steel side. It is also noted that the depth of attack in steel side is deeper close to the interfacial area than away from interface.

Figure 6 displays microstructure features of the titanium/steel joint after potentiodynamic polarization tests. The variation in the corrosion data of the joint brazed with different brazing parameters can be attributed to the developing microstructure and the particular behavior of the elements of the brazing alloy. Corrosion attack was concentrated at the steel

Table 4 Summary of the electrochemical data obtained in the corrosion tests

Joint	Open circuit potential, mV	Potential at current = 0, mV	Corrosion current density, μA/cm^2	Polarization resistance, Ω·cm^2	Corrosion rate, mm/year
Ti/St-930-15	−47.66	−46.21	182.67	139.80	1.94
Ti/St-970-15	−47.21	−47.84	41.91	307.80	0.9
Ti/St-1000-15	−46.86	−48.01	39.55	467.98	0.42
Cu-based filler	−12.50	−02.18	12.96	4141.03	0.28
CP Ti	14.20	30.73	0.11	8688.50	0.03
Steel	−47.70	−46.10	749.59	37.08	9.79

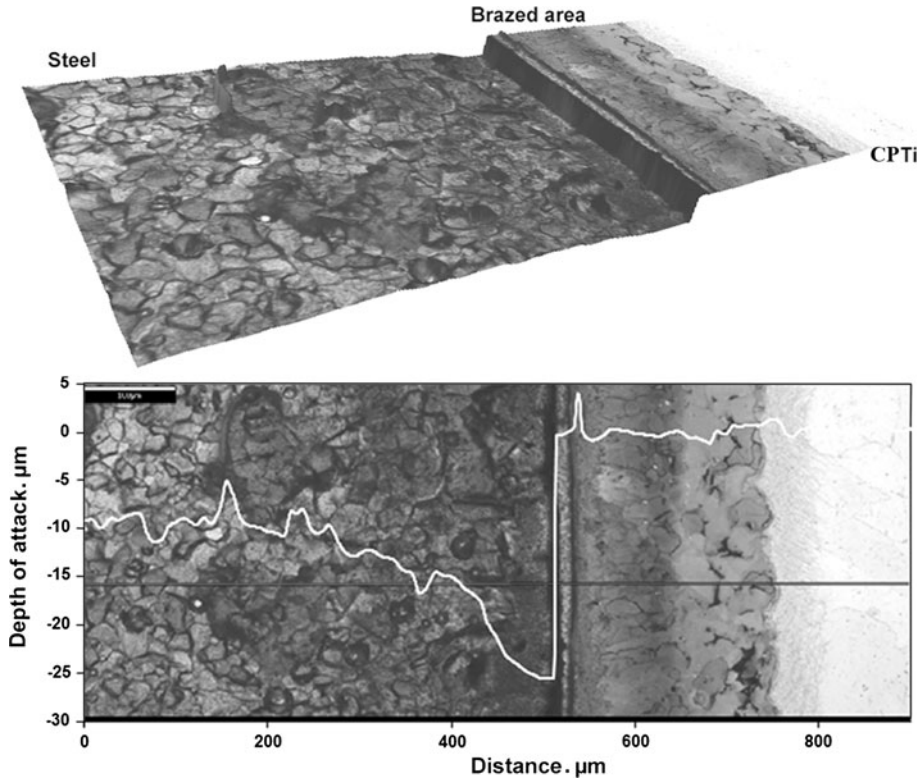

Fig. 4 Morphology of Ti/St-930-15 joint after performing potentiodynamic polarization experiment

side of the joint. Corrosion products were rich in sulfur and oxygen since corrosion of steel by sulfuric acid results in the evolution of hydrogen and the formation of iron sulfate. Corrosion resistance was low in case of joint brazed at a temperature of 930 °C owing to the presence of extensive voids in addition to the selective attack of $Ti45Cu_{55-x}Fe_x$ phase in the microstructure as it is clearly presented in Fig. 6(a) and the enlarged view Fig. 6(b). This phase is selectively dissolved and actively corroded in the used solution and converted into copper sulfide and copper oxide (Ref 8-11). Chemical analysis of the corroded microstructure has proved the presence of rather high content of sulfur and oxygen at this phase meanwhile, copper is clearly depleted from this area. Brazed area, adjacent to this phase, tends to passivate and form dense protected layer.

It is suggested that the corrosion resistance of the joints brazed at high temperatures, 970 and 1000 °C, showed better performance because of the enrichment of the microstructure by titanium element which is per se noble element and constitutes a passive layer. The microstructure was mainly consisting of dense α-β Ti and (Fe,Cu)Ti with less content of copper which improves the corrosion resistance. Figure 6(c) presents the joint brazed at the temperature of 1000 °C after potentiodynamic polarization test, and the enlarged view of the brazed area is shown in Fig. 6(d).

3.4 Mass Loss Measurements

The results of the weight loss and the depth of the attack in the steel side are shown in Fig. 7. The measurements have primarily comparative value since the loss of weight and the depth of the attack were mainly concentrated in the steel side adjacent to the brazed interface and minute corrosion was observed in the titanium and filler metal area. Similar to the results obtained by potentiodynamic measurements, the highest corrosion mass loss and depth of attack were observed in the joint Ti/St-930-15. However, brazed at high temperature, the Ti/St-970-15 and Ti/St-1000-15 were more resistant to corrosion attack.

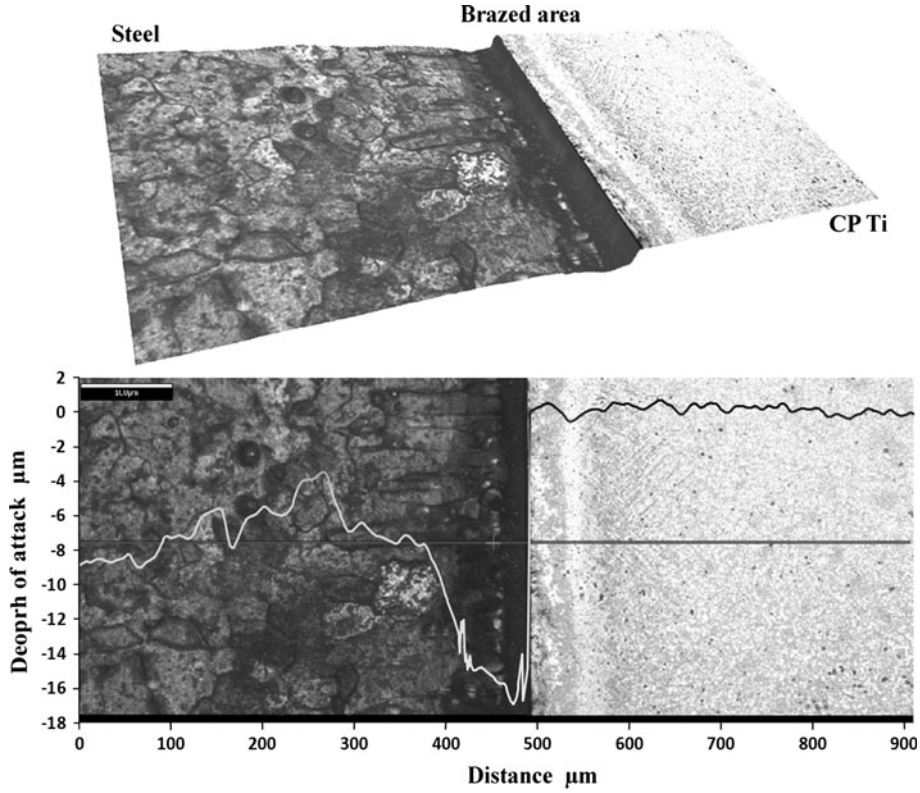

Fig. 5 Morphology of Ti/St-1000-15 joint after performing potentiodynamic polarization experiment

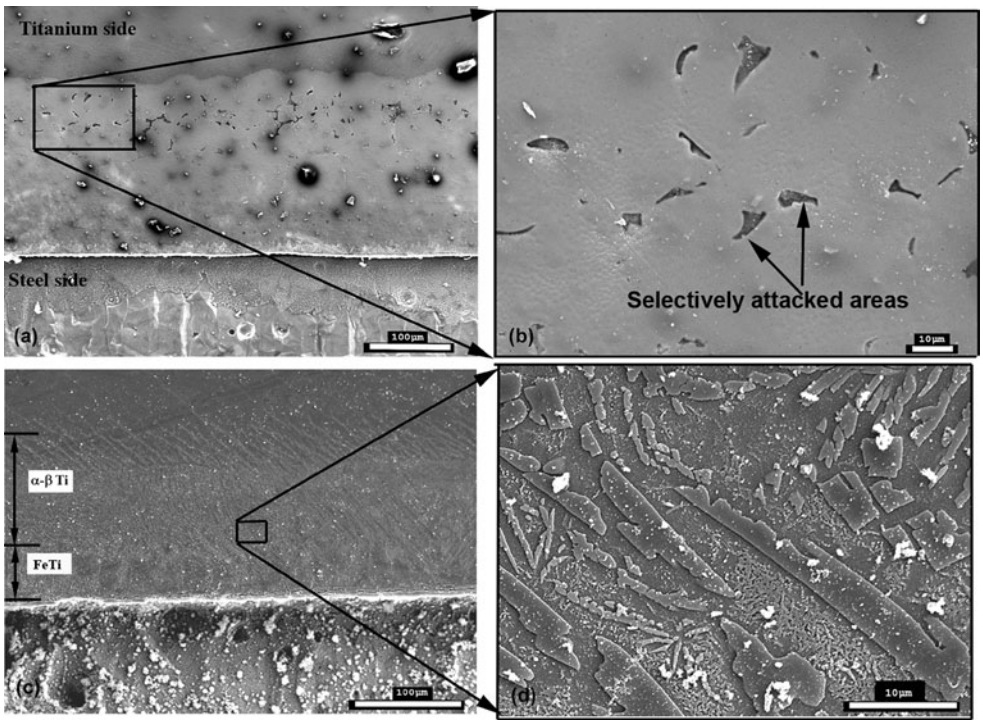

Fig. 6 Microstructure features of the titanium/steel joints after potentiodynamic polarization experiment: (a) SEM micrograph of Ti/St-930-15 joint, (b) close-up view of brazed area in Ti/St-930-15 joint, (c) SEM micrograph of Ti/St-1000-15 joint, and (d) close-up view of brazed area in Ti/St-1000-15 joint

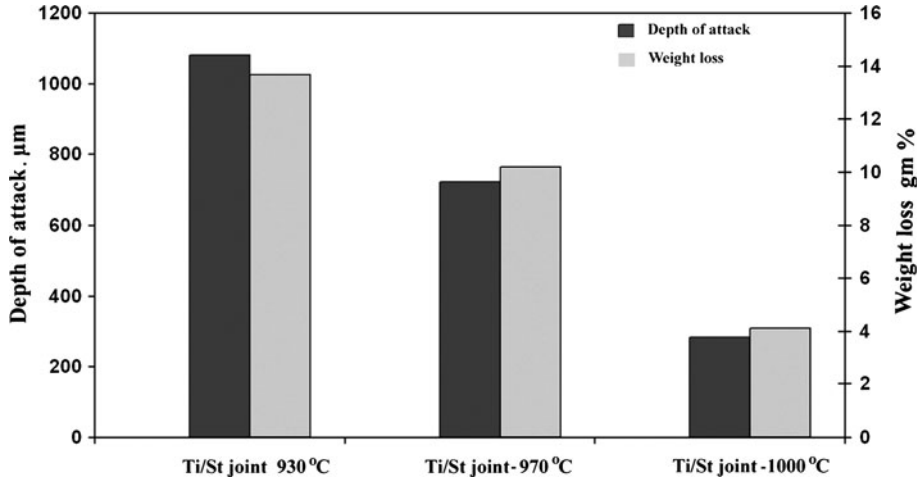

Fig. 7 The results of weight loss and the depth of attack measurements

4. Conclusions

The corrosion properties of the vacuum-brazed titanium and steel, using Cu-12Mn-2Ni filler alloys were extensively evaluated in this study. Important conclusions are summarized below:

1. The steel substrate showed a lower corrosion potential and a higher corrosion current density than the titanium substrate and the copper-based filler alloy. The maximum depth was measured in the case of joints brazed at the lowest brazing temperature (Ti/St-930-15), while the minimum was achieved in the case of joints brazed at the highest brazing temperature (Ti/St-1000-15).
2. Chemical analyses and the microstructure of the brazed area played a vital role in the corrosion resistance of the brazed joints. Joints brazed at the brazing temperature of 930 °C presented the lowest corrosion resistance owing to the presence of extensive voids in addition to the selective attack of $Ti45Cu_{55-x}Fe_x$ phase in the microstructure. Meanwhile, joints brazed at a temperature of 1000 °C give the best corrosion result owing to the high content of titanium in the microstructure which enables the formation of a passive rich film and the absence of voids and the harmful $Ti45Cu_{55-x}Fe_x$ phase in the microstructure.

References

1. O. Jinkeun, J.K. Nack, L. Sunghak, and W.L. Eui, Correlation of Fatigue Properties and Microstructure in Investment Cast Ti-6Al-4V Welds, *Mater. Sci. Eng.*, 2003, **A340**, p 232–242
2. H. Ozaki, R. Ichioka, T. Matsuura, and M. Kutsuna, Laser Roll Welding of Dissimilar Metal Joint of Titanium to Low Carbon Steel, *Mater. Sci. Forum*, 2008, **580–582**, p 543–546
3. F. Möller, M. Grden, C. Thomy, and F. Vollertsen, Combined Laser Beam Welding and Brazing Process for Aluminium Titanium Hybrid Structures, *Phys. Proc.*, 2011, **12**, p 215–223
4. J.G. Banker and J.P. Winsky, Titanium/Steel Explosion Bonded Clad for Autoclaves and Vessels, *ALTA Autoclave Design & Operation Symposium*, May 1999 (Melbourne), ALTA Metallurgical Services, 1999
5. A. Elrefaey and W. Tillmann, Characterization of Titanium/Steel Joints Brazed in Vacuum, *Weld. J.*, 2008, **87**, p 113s–118s
6. J.A. van Beek, A.A. Kodentsov, and F.J.J. van Loo, Phase Equilibria in the Cu-Fe-Ti System at 1123 K, *J. Alloys Compd.*, 1995, **217**, p 97–103
7. O.C. Paiva and M.A. Barbosa, Microstructure, Mechanical Properties and Chemical Degradation of Brazed AISI, 316 Stainless Steel/Alumina Systems, *Mater. Sci. Eng.*, 2008, **A480**(1–2), p 306–315
8. O.C. Paiva and M.A. Barbosa, Brazing Parameters Determine the Degradation and Mechanical Behaviour of Alumina/Titanium Brazed Joints, *J. Mater. Sci.*, 2000, **35**, p 1165–1175
9. L.S. Castleman and S.M. Motzkin, *Biocompatibility of Clinical Implant Materials*, CRC Press, Boca Raton, 1981
10. A. Elrefaey, L. Wojarski, and W. Tillmann, Investigation on Corrosion of Titanium/Steel Brazed Joint, *Materialwiss. Werkstoffiech*, 2010, **41**(11), p 908–913
11. H. Matsuoka, Y. Matsunaga, S. Mitsumoto, and H. Seki, Copper Corrosion and Capillary Action in Humid Atmospheres, *Corros. Eng.*, 1987, **36**, p 625–630